Environmental Science and Pollution Research (2020) 27:21299–21310
https://doi.org/10.1007/s11356-020-08612-8

RESEARCH ARTICLE

Sources and transformations of nitrate constrained by nitrate isotopes and Bayesian model in karst surface water, Guilin, Southwest China

Haijuan Zhao[1,2] · Qiong Xiao[2] · Ying Miao[2] · Zhijun Wang[2] · Qigang Wang[2]

Received: 9 October 2019 / Accepted: 26 March 2020 / Published online: 8 April 2020

Abstract

Surface water suffering from nitrate (NO_3^-) contamination in karst area is not only harmful to human health as drinking water but can also affect the process of carbonate rock weathering, so it is crucial to trace the sources and transformations of NO_3^- in karst surface water. In this study, an investigation of water chemical data and NO_3^- isotopes ($\delta^{15}N$ and $\delta^{18}O$) was used to elucidate the transformations of NO_3^- and quantify a proportional apportionment of NO_3^- sources of individual potential sources (incl. soil organic nitrogen (SON), atmospheric precipitation (AP), manure and sewage wastes (M&S), and chemical fertilizer (CF)) in the Lijiang River (typical karst surface water), Guilin, Southwest China. $\delta^{15}N\text{-}NO_3^-$ and $\delta^{18}O\text{-}NO_3^-$ values of water samples from the Lijiang River range from 2.14 to 13.50‰ (mean, 6.59‰) and from − 2.44 to 6.97‰ (mean, 3.76‰), respectively. A positive correlation between Cl^- and NO_3^- but no correlations between NO_3^- and $\delta^{15}N\text{-}NO_3^-$ or $\delta^{18}O\text{-}NO_3^-$ are found and the $\delta^{18}O\text{-}NO_3^-$ values fitted the theoretical $\delta^{18}O\text{-}NO_3^-$ values produced from nitrification, suggesting that the genesis of NO_3^- in waters of the Lijiang River is affected by nitrification processes and the mixing process has a major effect on NO_3^- transportation. Results of the Bayesian stable isotope mixing model show that the M&S and SON are the main NO_3^- source through the whole year (accounting for ~ 61% and 65% of the total NO_3^- in the wet and dry season, respectively), followed by CF (~ 29%). Furthermore, we find that nitrification of nitrogen in fertilizers, soil, and manure and sewage can promote the carbonate rock weathering. The estimated contribution of such nitrification to the weathering of carbonate rocks accounts for about 11% of the total carbonate rock weathering flux (calculated by HCO_3^-) in the Lijiang River. This finding indicates that the weathering of carbonate rock is probably affected by nitrogen nitrification processes in karst catchment.

Keywords NO_3^- isotopes · Bayesian isotope mixing model · Nitrification · Carbonate rock weathering · Lijiang River · Karst surface water

Introduction

About 15% of the continent is karst areas and in many regions, the karst aquifers provide the only available groundwater for drinking water (Ford and Williams 2007). However, karst aquifers are particularly vulnerable to anthropogenic contamination, because of the development of conduit networks and sinkholes by which quickly respond to the contaminants from the surface can easily enter into the aquifer, especially during the rainfall events and in areas with concentrated anthropogenic inputs (Jiang 2013; Yue et al. 2015). Extensive anthropogenic activities, such as intensive agricultural activities, excessive application of chemical fertilizers and manure (Pastén-Zapata et al. 2014; Matiatos 2016), have made the transportation of N to rivers and streams increased from 34 Tg N $year^{-1}$ to 64 Tg N $year^{-1}$ over the twentieth century (Van Beek et al.

Responsible editor: Philippe Garrigues

Electronic supplementary material The online version of this article (https://doi.org/10.1007/s11356-020-08612-8) contains supplementary material, which is available to authorized users.

✉ Qiong Xiao
xiaoqiong@karst.ac.cn

[1] Chongqing Key Laboratory of Karst Environment, School of Geographical Sciences, Southwest University, Chongqing 400715, China

[2] Key Laboratory of Karst Dynamics, MLR & Guangxi, Institute of Karst Geology, Chinese Academy of Geological Sciences, Guilin 541004, China

2016). Nitrate (NO_3^-) is a main form of N in natural environments and high concentration of NO_3^- in water is harmful to human health and aquatic life (Comly 1945; Lee et al. 2008; Bu et al. 2017). Many studies reported that it can lead to methemoglobinemia for infants and liver cancer, gastric cancer, and hypertension for adults to drink water with high NO_3^- concentration for long time (Dalton 1995). Moreover, some studies have shown that nitrogen cycling is closely coupled with carbonate rock weathering in karst areas (Raymond et al. 2008; Perrin et al. 2008; Barnes and Raymond 2009; Gandois et al. 2011). Hence, it is important to trace the sources and transformations of NO_3^- in the surface water in order to provide insights into the water quality protection and better understand the influence nitrogen cycling on the process of carbonate rock weathering.

Since different NO_3^- sources such as soil organic nitrogen (SON), atmospheric precipitation (AP), manure and sewage wastes (M&S), and chemical fertilizer (CF) have distinct isotope ratios of nitrogen ($^{15}N/^{14}N$) and oxygen ($^{18}O/^{16}O$), a dual isotope approach ($\delta^{15}N\text{-}NO_3^-$ and $\delta^{18}O\text{-}NO_3^-$) has been used broadly to provide information on the origins and transformations of NO_3^- in a hydrosphere (Liu et al. 2006; Xue et al. 2012; Zhang et al. 2018). Commonly, the typical $\delta^{15}N\text{-}NO_3^-$ values of chemical fertilizer fall in the range of − 6–6‰ and 0–8‰ for soil organic nitrogen, and 4–25‰ for manure and sewage wastes (Kendall et al. 2008; Xue et al. 2009). The $\delta^{18}O\text{-}NO_3^-$ values of NO_3^- from nitrification of mineralized soil organic nitrogen, NH_4^+ in fertilizer and rain, and sewage and manure range from − 10 to 10‰ (Xue et al. 2009; Kelley et al. 2013; Qin et al. 2019), while $\delta^{18}O\text{-}NO_3^-$ values of synthetic nitrate fertilizer vary between 17 and 25‰ (Kendall et al. 2008). The $\delta^{15}N\text{-}NO_3^-$ and $\delta^{18}O\text{-}NO_3^-$ signatures of NO_3^- from atmospheric precipitation range from − 13 to 13‰ and from 25 to 75‰, respectively (Xue et al. 2009; Saccon et al. 2013). Numerous biogeochemical processes that occur in soils and aquatic environments can result in variable N and O isotope fractionation and these fractionations are complex. Main processes that shift NO_3^- isotopic signatures include assimilation during photosynthesis, nitrification processes of nitrogen from soil, manure and sewage wastes, and ammonium fertilizer, and microbial denitrification in anaerobic environments (Kendall et al. 2008; Soto et al. 2019).

The dual isotopic mixing model based on mass balance theory has been widely used to estimate the contributions of individual NO_3^- sources (Deutsch et al. 2006; Kaown et al. 2009; Li and Ji 2016). However, this mixing model does not take into account of several factors with substantial uncertainty, including (1) temporal and spatial variability in $\delta^{15}N\text{-}NO_3^-$ and $\delta^{18}O\text{-}NO_3^-$; (2) fractionation caused by denitrification; (3) many NO_3^- sources contributing to the mixture (number of sources > number of isotope + 1) (Moore and Semmens 2008; Xue et al. 2009). A Bayesian stable isotope mixing model has been applied successfully to quantify the contributions of different NO_3^- sources in surface water, ground water, and the atmospheric precipitation with the uncertainties mentioned above (Xue et al. 2012; Lu et al. 2015; Zong et al. 2017; Ogrinc et al. 2019). Hydrochemistry and other isotopes (e.g., NO_3^-, Cl^-, $^{18}O\text{-}H_2O$) can also provide important information to distinguish NO_3^- sources and the N cycling processes.

Lijiang River is the upper reaches of the Guijiang River, one of tributaries of the Pearl River, it is a typical carbonate basin, and has a wide distribution of typical peak forest and peak cluster landforms. The Lijiang River provides 81.6% of the drinking water for the people of Guilin city. Previous studies showed that NO_3^- was the main species of dissolved inorganic nitrogen in the Lijiang River (Shen et al. 2015). The drinking water treatment plants are very sensitive to changes of the source water quality (Ghodeif et al. 2017). However, few studies on the sources and fate of NO_3^- have been conducted in the Lijiang River. In this study, hydrochemistry, $\delta^{15}N\text{-}NO_3^-$, $\delta^{18}O\text{-}NO_3^-$, and other isotopes were measured in the water of Lijiang River, in order to (1) identify the main sources of NO_3^- and its transformation in the water of Lijiang River; (2) quantify a proportional apportionment of individual NO_3^- sources by using a Bayesian isotopic mixing model; (3) analyze the influence of nitrogen cycling on the process of carbonate rock weathering of surface water in karst areas.

Material and methods

Study area

The Lijiang River is located in the southwest China and it is one of tributaries of the Pearl River. Length and drainage area of the Lijiang River are 164 km and 5039.7 km^2, respectively. It originates from Maoershan Mountain in the northwest of Xing'an County, Guangxi, China, and flows through Xing'an County, Guilin city, and Yangshuo County (Fig. 1). The region of Lijiang River watershed is located in a mid-subtropical monsoon climate zone, with hot and rainy summers, and cold and dry winters. The annual average air temperature is about 19 °C and annual average rainfall is about 2000 mm. The rainfall in the Lijiang River is concentrated from March to August, accounting for 70 to 80% of the year, so this period is divided into the wet season, and the rest of the time is the dry season. The landscape of the whole basin consists of 76% forestland, 14% cropland, 6% urbanland, 3% gardenland, and 1% water (Lin and Chen 2016). The land use pattern showed great variations from the upper reach to the lower reach. Geologically, the mid-upper parts of the catchment are Silurian granites, Ordovician–Cambrian shales, and mud rocks intercalated with carbonate rocks. In contrast, the mid-lower part is dominated by Devonian carbonate rocks, so has a wide distribution of peak forest and peak cluster karst

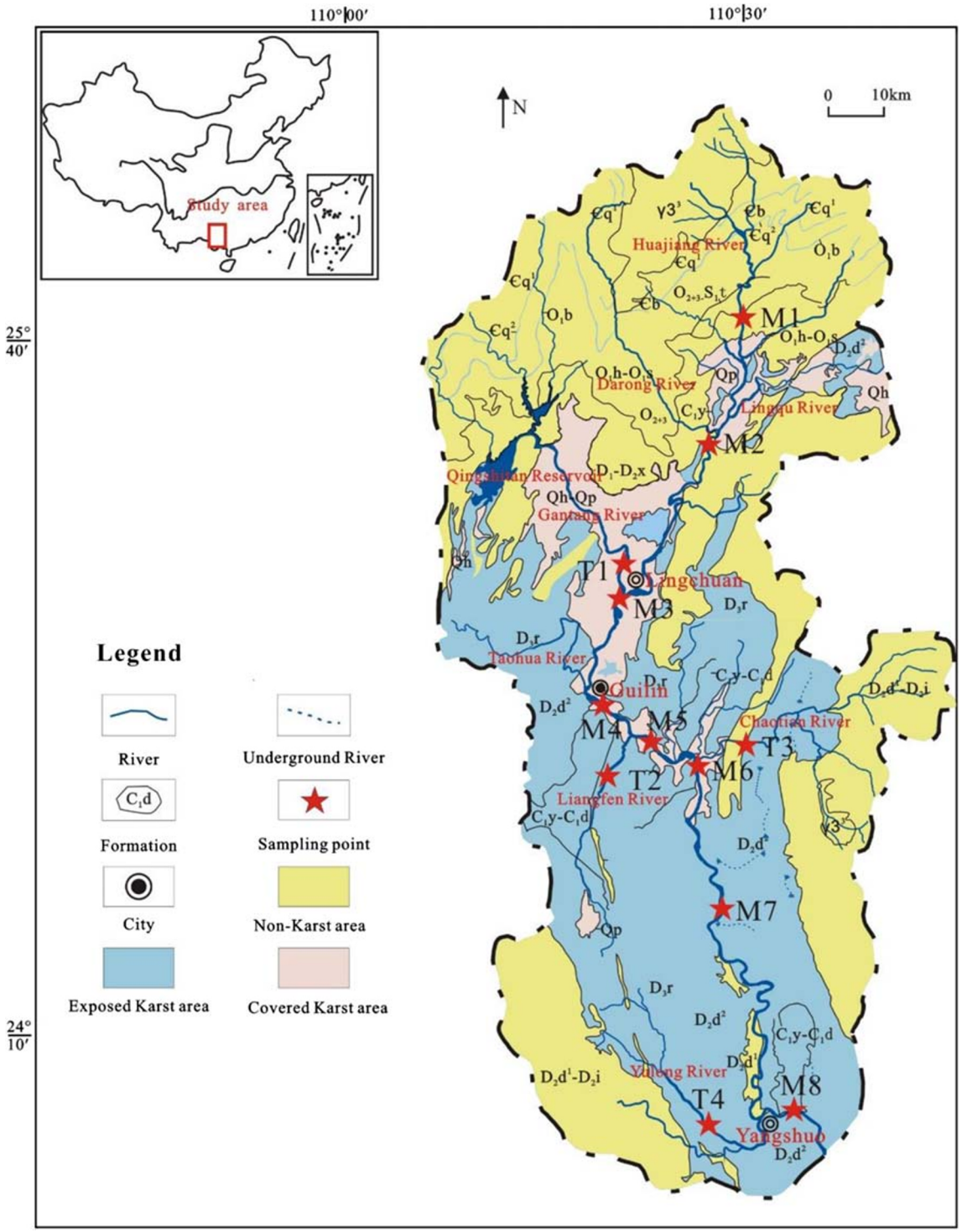

Fig. 1 Hydrogeological map of the study area showing the locations of sampling sites

landforms (Zhang et al. 2017). Agriculture is one of the pillar industries of Guilin city. More than 80% of Lijiang River Basin is agricultural area. Annual amount of N fertilizer application was approximately 7.03×10^5 kg year^{-1} between 2016 and 2017 in the Ginlin city (NBSC 1980-2018), and the main application of N fertilizer was urea, compound fertilizer, and ammonium bicarbonate (He 2013). At the same time, there is a lot of animal husbandry in rural areas of Guilin city, but there is no centralized treatment for scattered animal manure. Guilin city is also a famous tourist city. The Lijiang River is a world famous tourist attraction. According to statistics of Guilin Statistics Bureau, Guilin city received about 136.19 million tourists from all over the world between 2016 and 2017 (tjj.guilin.gov.cn/).

Sampling and analytical technique

Hydrochemistry

Eight sampling sites (including M1–M3 in the upper reach of Lijiang River, M4–M6 in the middle reach, M7 and M8 in the lower reach) along the mainstream of the Lijiang River and sites T1–T4 of four main tributaries near which they merge with the mainstream were chosen for water sample collection in this study (see the sampling locations in Fig. 1). Samples were collected monthly from July 2016 to June 2017. In the field, hydrochemical parameters including pH, water temperature (T), dissolved oxygen (DO), and electrical conductivity (EC) were measured by a multi-parameter water quality analyzer (YSI6920, USA) with precisions of 0.01 pH units, 0.01 °C, 0.01 mg L^{-1}, and 1 μS cm^{-1}, respectively. Water samples for the analyses of anions and cations were filtered through pre-combustion (450 °C, 12 h) glass fiber filters (Whatman, GF/F, 47 mm in diameter) and collected in pre-rinsed high-density polyethylene (HDPE) bottles (1 L). Samples for cation analysis were acidified to pH < 2 with HNO_3. The concentration of HCO_3^- was determined via HCl titration method with a Titrette Digital Titrator kit (Brand Trading Co., Ltd., Wertheim, Germany). The concentrations of anion NO_3^- and Cl^- were determined by ionic chromatography (ICS-900Thermo Fisher Scientific, USA). The concentrations of cation Ca^{2+} and Mg^{2+} were determined by ICP-OES (2100DV Perkin Elmer Inc., USA). Reported analytical uncertainties were within ± 5%. Data of monthly average discharge of the Lijiang River at site M8 were obtained from the Guilin Bureau of Hydrology and Water Resources (swszyj.gxzf.gov.cn/).

Isotopes

$\delta^{15}N\text{-}NO_3^-$, $\delta^{18}O\text{-}NO_3^-$, and $^{18}O\text{-}H_2O$ values of water samples were determined. The $^{18}O\text{-}H_2O$ values were determined with a liquid water stable isotope analyzer (LWIA-24-d, Los Gatos Research, USA). The analytical precision for $\delta^{18}O\text{-}H_2O$ was ± 0.2‰. The $\delta^{15}N\text{-}NO_3^-$ and $\delta^{18}O\text{-}NO_3^-$ were determined by a chemical conversion method. First, NO_3^- was reduced to NO_2^- by adding 0.8 mL of 20 g L^{-1} $CdCl_2$ solution, 0.8 mL of 250 g L^{-1} NH_4Cl solution, and clean zinc sheet to 40 mL water sample in headspace vials and then oscillating the headspace vials at 220 R min^{-1} on a shaker for 15 min. Second, NO_2^- reduced to N_2O with NaN_3 in an acetic acid buffer. Finally, N_2O was separated, purified using a Trace Gas Pre-concentrator unit (Isoprime Ltd., Cheadle Hulme, Cheadle, UK) after the injection of 0.1–0.2 mL of 10 mol L^{-1} NaOH solution to remove CO_2 gas and inhibit microbial activity(Casciotti et al. 2002). $\delta^{15}N$ and $\delta^{18}O$ of N_2O were measured using elemental analyzer interfaced with a MAT 253 isotope ratio mass spectrometry (Thermo Fisher Scientific, USA) at the State Oceanic Administration Third Institute of Oceanography, Xiamen, China. The international (USGS-32, USGS-34, USGS-35 and IAEA-N3) standards were used to calibrate the $\delta^{15}N\text{-}NO_3^-$ and $\delta^{18}O\text{-}NO_3^-$ values of samples (Casciotti et al. 2002). The analytical precision for $\delta^{15}N\text{-}NO_3^-$ and $\delta^{18}O\text{-}NO_3^-$ was ± 0.2‰ and ± 0.3‰, respectively. $\delta^{15}N\text{-}NO_3^-$ was reported relative to N_2 in the atmosphere. Vienna Standard Mean OceanWater (VSMOW) is standard for $\delta^{18}O\text{-}H_2O$ and $\delta^{18}O\text{-}NO_3^-$.

Estimation of the contributions of individual nitrate sources

The contribution of potential NO_3^- sources to NO_3^- in surface water can be quantified by a Bayesian mixing model (Parnell et al. 2010, 2013). The mixing model has been implemented using a "SIAR" (Stable Isotope Analysis in R) software package and has been successfully used to estimate the contributions of multiple NO_3^- source (Ding et al. 2014; Liu et al. 2018b; Zhang et al. 2018).

$$\begin{aligned} X_{ij} &= \sum_{k=1}^{k} P_k\left(S_{jk} + C_{jk}\right) + \varepsilon_{ij} \\ S_{jk} &\sim N\left(\mu_{jk}, \omega_{jk}^2\right) \\ C_{jk} &\sim N\left(\lambda_{jk}, \tau_{jk}^2\right) \\ \varepsilon_{ij} &\sim N\left(0, \sigma_j^2\right) \end{aligned} \quad (1)$$

In Eq. (1), X_{ij} is the isotope value j of the water sample i; S_{jk} is the source value k of isotope j ($k = 1, 2, 3,., K$) and is normally distributed with mean μ_{jk} and standard deviation (SD) ω_{jk}; p_k is the proportion of source k, which needs to be estimated using the SIAR model; c_{jk} is the fractionation factor for isotope j on source k and is normally distributed with mean λ_{jk} and SD τ_{jk}; and ε_{ij} is the residual error representing additional unquantified variation between individual mixtures and is normally distributed with mean 0 and SD σ_j. A detailed description of this model can be found in Parnell et al. 2010.

To estimate the contributions of NO_3^- sources in the Lijiang River, $\delta^{15}N\text{-}NO_3^-$ and $\delta^{18}O\text{-}NO_3^-$ ($j = 2$) and four potential sources (SON, AP, M&S, and CF) were applied as specific isotope values in this study. These potential source values were obtained from previously published literature (Table 1). C_{jk} was set as zero based on the discussion in the "Seasonal and spatial changes of nitrate isotopic compositions of water samples from the Lijiang River" section. The Shapiro-Wilk test was used to examine the normality of the potential source values.

Calculations

The annual NO_3^- flux (F_{NO3}) was estimated using the monthly NO_3^- concentration (C_m) and monthly average

Table 1 $\delta^{15}N$ and $\delta^{18}O$ values of various NO_3^- sources

Sources	n	$\delta^{15}N\text{-}NO_3^-$ (‰)	$\delta^{18}O\text{-}NO_3^-$ (‰)	Literatures
SON	6	5.7 ± 2	1.24 ± 3.13	(Liu et al. 2006; Lu et al. 2015)
AP	8	3.1 ± 1.5	56.7 ± 17.8	(Ding et al. 2014; Li et al. 2018)
M&S	16	14.3 ± 1.9	6.7 ± 2.5	(Xian et al. 2016)
CF	6	− 1.12 ± 1.41	− 5.7 ± 1.7	(Liu et al. 2006; Li et al. 2018)

discharge (Q_m) at the mouth of the Lijiang River as follows:

$$F_{NO3} = \sum_m C_m \times Q_m \quad (2)$$

where the annual NO_3^- flux (F_{NO3}) is the sum of monthly flux of NO_3^- during one hydrological year; Q_m represents the monthly average discharge at the river mouth (Table 2), in which $m = 1, 2, 3, \ldots, 12$; C_m denotes the monthly NO_3^- concentration at the river mouth.

Theoretical $\delta^{18}O\text{-}NO_3^-$ from nitrification. When nitrification occurs, the theoretical $\delta^{18}O\text{-}NO_3^-$ can be calculated using the following equation (Boshers et al. 2019)

$$\begin{aligned}\text{Theoretical } \delta^{18}O\text{–}NO_3^- &= \left(\frac{2}{3}+\frac{1}{3}X_{NO2,T}\right)\delta^{18}O\text{–}H_2O \\ &+\frac{1}{3}\left[\left(\delta^{18}O_{O2}-{}^{18}\varepsilon_{k,O2}-{}^{18}\varepsilon_{k,H2O,1}\right)\left(1-X_{NO2,T}\right)-{}^{18}\varepsilon_{k,H2O,2}\right] \\ &+\frac{2}{3}\left(X_{NO2,T}\,{}^{18}\varepsilon_{eq}\right)\end{aligned} \quad (3)$$

where theoretical $\delta^{18}O\text{-}NO_3^-$ is the theoretical $\delta^{18}O\text{-}NO_3^-$ value of NO_3^- when nitrification occurs, $\delta^{18}O\text{-}H_2O$ is the $\delta^{18}O$ value in the water and $\delta^{18}O_{O2}$ is the $\delta^{18}O$ value of atmospheric O_2. ${}^{18}\varepsilon_{k,O2}$ is the kinetic isotope effect for O_2 incorporation, ${}^{18}\varepsilon_{k,H2O,1}$ is the kinetic isotope effect for H_2O incorporation during nitrite (NO_2^-) production, ${}^{18}\varepsilon_{k,H2O,2}$ is the kinetic isotope effect associated with O atom incorporation from water into NO_2^- during oxidation to NO_3^-, ${}^{18}\varepsilon_{eq}$ is equilibrium isotope fractionation factor between NO_2^- and H_2O, and $X_{NO2,T}$ is the fraction of NO_2^- O atoms that have exchanged with H_2O during NO_2^- production. According to the research of Boshers et al. (2019), the values of ${}^{18}\varepsilon_{k,O2}$ + ${}^{18}\varepsilon_{k,H2O,1}$, ${}^{18}\varepsilon_{k,H2O,2}$, ${}^{18}\varepsilon_{eq}$, and $X_{NO2,T}$ are 27.3‰, 13.5‰, 13‰, and 78%, respectively.

Results

Seasonal and spatial variations of water chemistry in the Lijiang River

The data of physical, chemical, and isotopic values for water samples from the Lijiang River are listed in Table S1. Results show that water temperature at all sampling sites ranged from 10.48 to 33.90 °C and had a seasonal variation with high values in the wet season (mean, 22.70 °C) and low values in the dry season (mean, 17.11 °C). The river water was neutral to alkaline (pH, 6.94–9.15) and the mean pH value was 7.60 in the wet season and 7.96 in the dry season. The DO ranged from 5.93 to 15.86 mg L^{-1} with an average of 9.57 mg L^{-1}, and there were no significant seasonal and spatial difference in the DO values. The EC values varied from 31.23 to 450.80 μS cm^{-1} and had a seasonal variation with low values in the wet season (188.40 μS cm^{-1}) and high values in the dry season (219.03 μS cm^{-1}). The EC values increased from the upper reach to the lower reach.

The hydrochemical type of river water is of HCO_3-Ca type, and HCO_3^- and Ca^{2+} are main ions. The HCO_3^- and Ca^{2+} concentrations ranged from 12.20 to 231.80 mg L^{-1} and from 5.49 to 77.94 mg L^{-1}, with an average of 106.83 mg L^{-1} and 35.75 mg L^{-1}, respectively. The HCO_3^- and Ca^{2+} concentrations were higher in the dry season than that in the wet season, and both increased from the upper reach to the lower reach (Fig. 2). The spatial variation in HCO_3^- and Ca^{2+} concentrations along the mainstream was lower than those of the

Table 2 Monthly average discharge data at the Lijiang River mouth

Time	2016 − 07	2016 − 08	2016 − 09	2016 − 10	2016 − 11	2016 − 12	2017 − 01	2017 −02	2017 − 03	2017 − 04	2017 − 05	2017 − 06
Discharge (m^3 s^{-1})	267	163	90.8	55.2	56.6	51.2	58.1	59.7	214	228	283	556

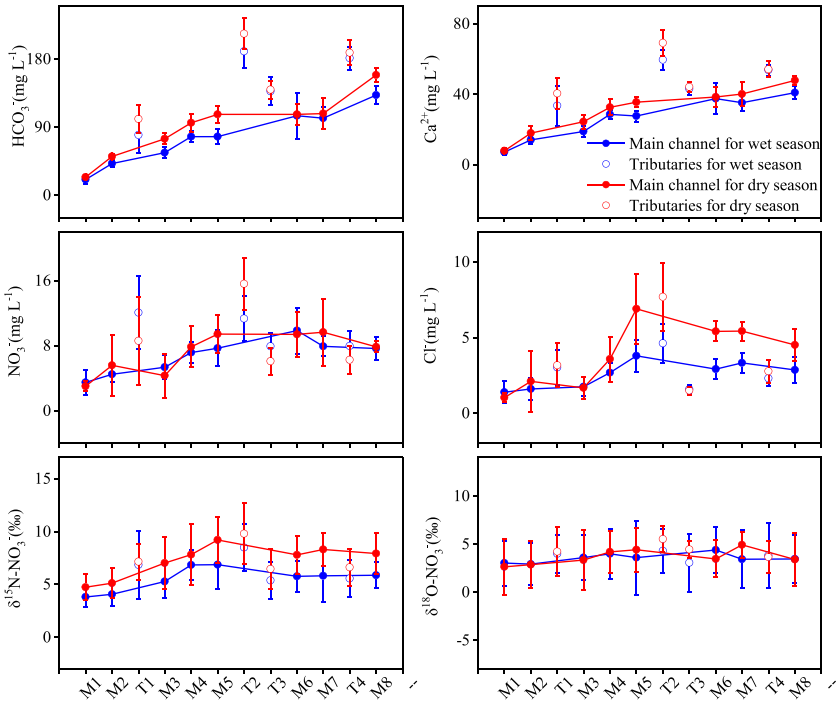

Fig. 2 Spatio-temporal variations of main ions, δ^{15}N-NO_3^- and δ^{18}O-NO_3^- (mean ± SD) values of water samples from the main stream and tributaries of the Lijiang River

tributaries in the upper reach of Lijiang River. A wide range of NO_3^- concentrations were observed in the Lijiang River, the NO_3^- concentrations varied from 0.39 to 19.42 mg L^{-1} with an average of 7.73 mg L^{-1} in the wet season and 7.80 mg L^{-1} in the dry season. There were significant spatial variations for the NO_3^- concentrations along the mainstream of Lijiang River which increased from the upper reach to the lower reach. High NO_3^- concentrations were observed in the tributary water samples T1 and T2. However, no significant difference in NO_3^- concentrations was found between both wet and dry seasons, and the mean values of NO_3^- showed relatively high standard deviations in the dry season, especially at sites M2, M7, T1, and T2. Concentrations of Cl^- at all sampling sites ranged from 0.27 to 11.08 mg L^{-1}, with low values in the wet season (mean, 2.64 mg L^{-1}) and high values in the dry season (mean, 3.81 mg L^{-1}). The mean values of Cl^- showed relatively high standard deviations in the dry season, especially at sites M2, M5, and T1. Spatially, the mean Cl^- concentration increased from the upper reach to the lower reach, and high Cl^- concentration was observed in T2 (Fig. 2).

Seasonal and spatial changes of nitrate isotopic compositions of water samples from the Lijiang River

The δ^{15}N-NO_3^- values ranged from 2.14 to 13.50‰ with a mean value of 6.59‰. The mean values of δ^{15}N-NO_3^- showed a seasonal variation with low values in the wet season (5.87 ± 1.12 °C) and high values in the dry season (7.72 ± 2.35 °C). The mean values of δ^{15}N-NO_3^- were higher in the middle reach than in the upper reach and the lower reach in both dry and wet seasons (Fig. 2).

The δ^{18}O-NO_3^- values was between − 2.44 and 6.97‰ with an average of 3.61‰ in the wet season and between − 1.21 and 6.87‰ with an average of 3.93‰ in the dry season. The seasonal variation of the mean values of δ^{18}O-NO_3^- was not significant. There was little spatial variation in both wet and dry seasons.

Discussion

NO_3^- sources identified by isotopes and hydrochemistry

NO_3^- in surface water could be derived from SON, M&S, CF, and AP. The dual isotope approach is used to trace the NO_3^- sources as different NO_3^- sources and different isotopic compositions. Figure 3 shows the δ^{15}N-NO_3^- and δ^{18}O-NO_3^- values of water samples from the Lijiang River and typical isotopic ranges for different sources. As indicated in Fig. 3, almost all of δ^{15}N-NO_3^- and δ^{18}O-NO_3^- values fall within the ranges of CF, SON and M&S source category, suggesting that the CF, SON, and M&S are the main sources of NO_3^- in the Lijiang River.

Chloride is a good indicator of manure and sewage input and rainwater dilution because it is inert to physical, chemical, and microbiological processes (Liu et al. 2006). The ratio of NO_3^-/Cl^- can provide more information to distinguish the effect of dilution from denitrification on N removal processes

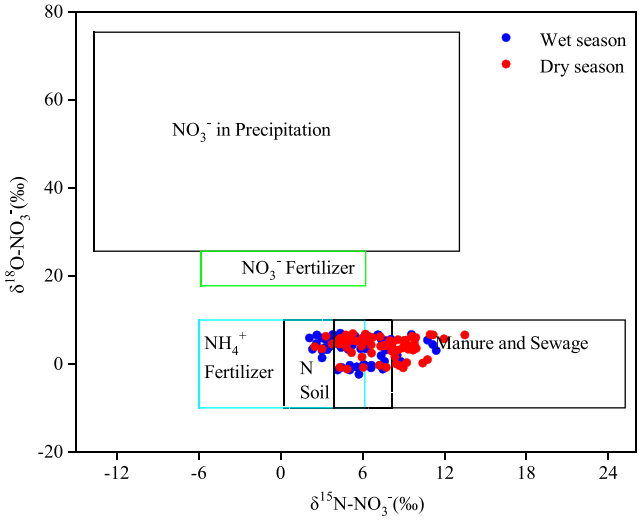

Fig. 3 Cross-plot of $\delta^{15}N\text{-}NO_3^-$ and $\delta^{18}O\text{-}NO_3^-$ values of water samples from the Lijiang River. The typical NO_3^- end members are adapted from (Kendall et al. 2008; Xue et al. 2009; Pernet-Coudrier et al. 2012)

(Liu et al. 2006, 2018a; Lu et al. 2015). The influence of evaporite weathering on Cl^- concentrations should be considered before using NO_3^-/Cl^- ratios to identify NO_3^- sources since evaporate, like halite, could contribute to Cl^- in river water (Li et al. 2018). However, the evaporites are not found in the Lijiang watershed (Yuan 2016). In the investigated water samples, positive correlations between Cl^- and NO_3^- were observed in the wet season ($R^2 = 0.44$) and in the dry season ($R^2 = 0.64$), indicating that the mixing process has occurred during the NO_3^- transportation in the Lijiang River (Fig. 4a). Different NO_3^- sources have varied levels of NO_3^-/Cl^- ratios, and the source of chemical fertilizers is characterized by high NO_3^-/Cl^- ratios and low concentrations of Cl^-, while municipal sewage has a significantly high Cl^- concentration and low NO_3^-/Cl^- ratio (Widory et al. 2005). Figure 4 b shows the variation of the NO_3^-/Cl^- molar ratios relative to Cl^- concentrations that varied widely from 0.86 to 3.11 with an average of 1.82 in the wet season and from 0.52 to 2.78 with an average of 1.36 in the dry season, which suggests a mixture of multiple sources of NO_3^-, including chemical fertilizers, soil nitrogen, municipal sewage, and animal waste. The NO_3^-/Cl^- molar ratios for most samples in the wet season had higher values than those in the dry season, suggesting that some potential NO_3^- input into the surface water might have been ascribed to precipitation, fertilizer application, and nitrification of soil nitrogen in the wet season. It has been reported that municipal sewage has a significantly high Cl^- concentration but very low NO_3^-/Cl^- ratio (Liu et al. 2006), indicating that NO_3^- from municipal sewage in the dry season was higher than that in the wet season in this study.

Transformations of NO_3^- in the Lijiang River

The isotopic compositions of NO_3^- are governed by isotope fractionation during physical and biogeochemical processes, such as assimilation, nitrification, and denitrification; thus, the NO_3^- derived from various potential sources has distinct isotopic values (Kendall et al. 2008). For an instance, the nitrification process results in depleted $\delta^{15}N\text{-}NO_3^-$ values; however, the denitrification and NO_3^- assimilation by phytoplankton lead to an increase in $\delta^{15}N\text{-}NO_3^-$ and $\delta^{18}O\text{-}NO_3^-$ values because lighter isotopes ^{14}N and ^{16}O are preferentially metabolized by microorganisms or phytoplankton (Sigman et al. 2005, 2008; Chen et al. 2019).

No correlations between NO_3^- and $\delta^{15}N\text{-}NO_3^-$ or $\delta^{18}O\text{-}NO_3^-$ of water samples from Lijiang River were discovered, suggesting that there were multiple biogeochemical processes affecting the distribution of NO_3^- in the river. During the nitrification process, ammonium is oxidized to NO_3^- by nitrifying bacteria ($2NH_4^+ + 3O_2 \rightarrow 2NO_2^- + 2H_2O + 4H^+$; $2NO_2^- + O_2 \rightarrow 2NO_3^-$) (Andersson and Hooper 1983). According to the research of Boshers et al. (2019), the theoretical $\delta^{18}O\text{-}NO_3^-$ can be calculated by the Eq. 3 during the nitrification process, a linear formulation of the theoretical $\delta^{18}O\text{-}NO_3^-$ versus $\delta^{18}O\text{-}H_2O$. The $\delta^{18}O\text{-}H_2O$ values of water samples from the Lijiang River ranged from −7.21 to −

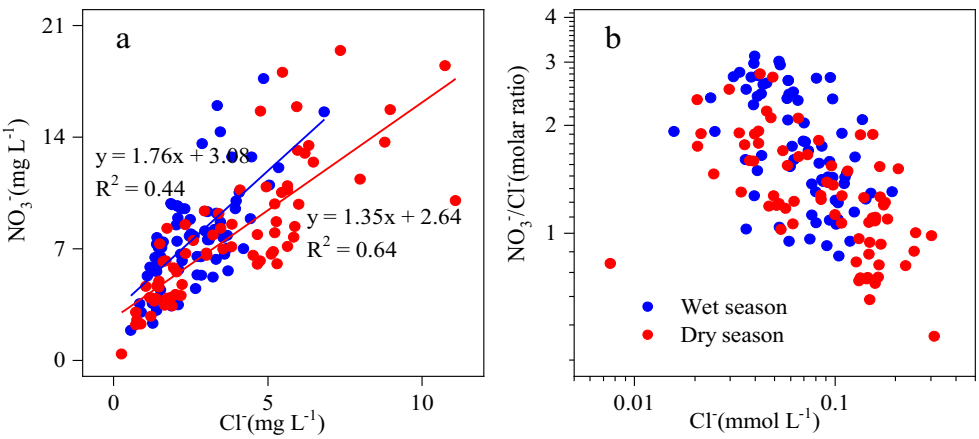

Fig. 4 **a** Relationship between Cl^- and NO_3^- concentrations, and **b** relationship between Cl^- mmolar concentration and NO_3^-/Cl^- molar ratio of water samples from the Lijiang River

3.53‰, and the $\delta^{18}O$ value of atmospheric O_2 is 23.9‰ (Barkan and Luz 2005). Hence, the theoretical $\delta^{18}O\text{-}NO_3^-$ values produced from nitrification would have a range from 0.08 to 3.47‰. As shown in Fig. 5, most of $\delta^{18}O\text{-}NO_3^-$ values were higher than the theoretical $\delta^{18}O\text{-}NO_3^-$ range, which may be related to several factors, such as the variable ratio of oxygen from the air and water, oxygen isotope fractionation, and different biological processes (Mayer et al. 2001). Kendall et al. (2008) found that the $\delta^{18}O$ of O_2 produced by the bacterial respiration and the evaporated H_2O in soil can result in high $\delta^{18}O$ values in NO_3^-. Some $\delta^{18}O\text{-}NO_3^-$ values were lower than theoretical values in the rainy season (Fig. 5), which possibly suggests that more O in NO_3^- are from unevaporated H_2O in soil into NO_3^- in the nitrification process. Moreover, the $\delta^{18}O\text{-}NO_3^-$ values of water samples from the Lijiang River were in the range of − 10 to + 10‰, and such $\delta^{18}O\text{-}NO_3^-$ signatures reflect the influence by nitrification (Kendall et al. 2008). It could thus be concluded that the NO_3^- of water samples from the Lijiang River is dominantly affected by nitrification process.

Denitrification is an important process mechanism for the reduction of NO_3^- via the transformation of NO_3^- to N_2O or nitrogen gas (N_2) under anoxic conditions, where dissolved oxygen concentrations are less than 2 mg L^{-1} (Rivett et al. 2008), resulting in the enrichment of isotopic values for the remaining NO_3^- (Xue et al. 2009). A linear relationship between $\delta^{15}N\text{-}NO_3^-$ relative to $\delta^{18}O\text{-}NO_3^-$ with the slopes of 0.48–0.76 is observed by an indicative of denitrification (Fukada et al. 2003; Xue et al. 2009). In this study, the slopes of $\delta^{15}N\text{-}NO_3^-$ relative to $\delta^{18}O\text{-}NO_3^-$ for the Lijiang River were − 0.41 and 0.17 in the wet season and dry season, respectively, both which are out of range of 0.48–0.76 that are associated with denitrification. Furthermore, the DO concentrations are 5.93–15.86 mg L^{-1} during the period of study, also indicating that the denitrification effects are not significant in the Lijiang River. Assimilation of NO_3^- during the photosynthetic process can cause a large shift in the 1:1 relationship between the $\delta^{15}N\text{-}NO_3^-$ and $\delta^{18}O\text{-}NO_3^-$. As mentioned above, the slopes of $\delta^{15}N\text{-}NO_3^-$ relative to $\delta^{18}O\text{-}NO_3^-$ were not around 1, but DO concentration is high, which suggests that assimilation maybe not significant but more obvious than denitrification in the Lijiang River.

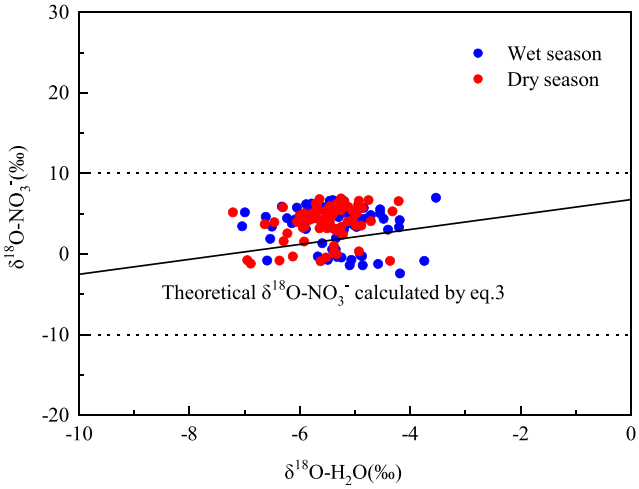

Fig. 5 Relationship between $\delta^{18}O\text{-}NO_3^-$ and $\delta^{18}O\text{-}H_2O$ of water samples from the Lijiang River

Contributions of individual NO_3^- sources estimated using SIAR

The ranges of the contributions of each NO_3^- source calculated using the SIAR model are shown in Fig. 6, and all of these four potential NO_3^- sources showed seasonal and spatial variations in the Lijiang River. During the wet season, the four potential NO_3^- sources including CF, SON, M&S, and AP contributed 31.63%, 32.45%, 28.46%, and 7.46%, respectively. During the dry season, M&S was the dominant NO_3^- source with a contribution of 36.45%, followed by SON (mean, 28.89%), CF (mean, 26.46%), and AP (mean, 8.20%). Overall, CF, M&S, and SON are the main NO_3^- sources in waters of the Lijiang River, and this finding is consistent with the results qualitatively determined via the dual isotopic method.

There are significant spatio-temporal variations in the contribution of SON. Compared with that in the dry season, SON inputs increased by around 4% in the wet season, which might be attributed to more flushing of SON from hill slopes to rivers under the intense rainfall conditions (Li et al. 2018). The SON contribution increased by around 3% from upstream to downstream in the wet season, which maybe relate to the extent of soil erosion. The soil erosion in the Lijiang River Basin has obvious differences between karst area and non-karst area. The soil erosion in the karst area is moderate and extremely strong, which accounts for 53% of the entire karst

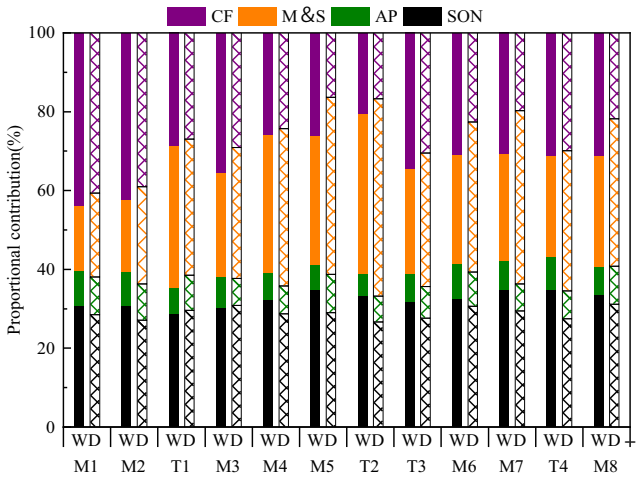

Fig. 6 Seasonal and spatial variation of proportional contributions (mean probability estimate) of NO_3^- sources in the Lijiang River estimated by SIAR. W represents the wet season, D represents the dry season

area, while moderate and medium soil erosion area in the non-karst area accounts for 12.4% and 10.4% of the total non-karst area, respectively (Qin et al. 2018). The upper reach is non-karst area, while the mid-lower reach is karst area (Fig. 1). However, the spatial variation of SON contribution was not significant in the dry season.

Owing to the heavy application of N fertilizer (7.03×10^5 kg year^{-1} between 2016 and 2017 (NBSC 1980-2018)) in the Ginlin city, China, the CF is one of the dominant sources of NO_3^- at all sampling sites. The contribution of CF was much higher in the wet season than in the dry season, indicating that a runoff flushing effect on fertilizer cannot be ignored. The CF contribution in the upstream was 8–10% higher than that in the mid-lower stream, which may be related to more cropland in the upstream. The area of cropland in the upper reaches of the Lijiang River Basin is 9% higher than that in the middle and lower reaches (Lin and Chen 2016).

M&S is one of the dominant NO_3^- source in the Lijiang River, and the contribution of it in the mid-lower stream was 5–11% higher than that in the upstream, which may be related to more intense human activity in the mid-lower stream. The area of urbanland in the middle and lower reaches of the Lijiang River Basin is 5% higher than that in the upper reaches (Lin and Chen 2016). The contribution of M&S in the dry season was about 8% higher than that in the wet season. It was noted that high NO_3^- concentrations in the tributary water samples were detected (T2) in which the contribution of M&S can reach up to 50%.

Atmospheric precipitation contributed the least NO_3^- in the whole watershed of the Lijiang River, which is in agreement with other river watersheds (Xue et al. 2012; Li et al. 2018). AP contributed 7.46% NO_3^- during the dry season and 8.20% during the wet season. Moreover, the contribution of AP in upstream is similar to that in the mid-lower stream of Lijiang River in both the dry and wet seasons.

As shown in Fig. 7, the NO_3^- concentrations were about 3 mg L^{-1} in the headstream (M1), about 9 mg L^{-1}in the midstream (M6) where the activities of human beings become intense and keep about 7 mg L^{-1} in the outlet (M8). The increase of NO_3^- downstream is mainly due to the increase of M&S, especially at sites T2 where the NO_3^- concentrations were the highest in the Lijiang River. Meanwhile, the contribution of M&S to NO_3^- can be up to 40–50%. In all, CF and M&S were the dominant NO_3^- source in the Lijiang River. Hence, some measures should be taken to alleviate NO_3^- pollution. For an example, fertilizer application must be properly reduced according to the soil nutrients and crop demands, and diffused domestic waste water should be collected by sewage treatment plant.

NO_3^- exported from the Lijiang River

The results show that NO_3^- flux in the Lijiang River was 4.10×10^7 kg year^{-1} calculated by the NO_3^- concentration and average monthly discharge rate of river flow (Eq. 2). The Lijiang River is one of tributaries of the Xijiang River. According to the research of Li et al. (2018), the NO_3^- flux was 9.21×10^8 kg year^{-1} in the Xijiang River. The NO_3^- flux of the Lijiang River accounted for about 5% of that in the Xijiang River. The NO_3^- flux of the Lijiang River during the wet season (3.35×10^7 kg) was approximately 4.5 times higher than that during the dry season (7.52×10^6 kg), which indicates about 82% NO_3^- transportation occurs during the wet season. The contributions of CF and M&S to NO_3^- were 60.09% and 62.91% in the wet season and dry season, respectively. Thus, in the study area, 60.61% of the NO_3^- flux was derived from anthropogenic activities.

Nitrification and carbonate rock weathering in the Lijiang River

In karst area, carbonate rock weathering is the main source of ions in rivers, and HCO_3^- in rivers is mainly derived from carbonated weathered carbonate rock (Gaillardet et al. 1999). Carbonate rock dissolved by carbonic acid, the equivalent ratios of $[Ca^{2+}+Mg^{2+}]/[HCO_3^-]$ should be 1 (Eq. 4). The equivalent ratio of $[Ca^{2+}+Mg^{2+}]$ /$[HCO_3^-]$ ranged from 1.08 to 1.37, with an average of 1.20, indicating that exogenous acid (sulfuric acid and nitric acid) weathered carbonate rock. Barnes and Raymond (2009) found that the acid produced during nitrification can take part in the dissolution of carbonate rocks, resulting in increased DIC in river water (Eq. 5).

$$Ca_xMg_{(1-x)}CO_3 + H_2CO_3 \rightarrow xCa^{2+} + (1-x)Mg^{2+} + 2HCO_3^- \quad (4)$$

$$NH_4^+ + 2O_2 + 2Ca_xMg_{(1-x)}CO_3 \rightarrow NO_{3-} + 2xCa^{2+} + 2(1-x)Mg^{2+} + 2HCO_3^- + H_2O \quad (5)$$

As stated above, NO_3^- in the Lijiang River mainly comes from nitrification of fertilizers, soil, and manure and sewage (92.54% and 91.80% in the wet and dry season, respectively). Thus, nitrification would enhance carbonate rock weathering in karst areas (Eq. 5). One mole of NO_3^- from nitrification would produce two moles of HCO_3^- and would be produced by carbonate rock weathering (Eq. 5). The increased HCO_3^- flux was 7.81×10^7 kg yearr^{-1} from nitrification of fertilizers, soil, and manure and sewage in the Lijiang River. HCO_3^- flux caused by nitrification accounted for 10.62% of the total HCO_3^- flux in the Lijiang River. This value was comparable with the calculation conducted by Yue et al. (2015), which showed that the HCO_3^- flux caused by nitrification was

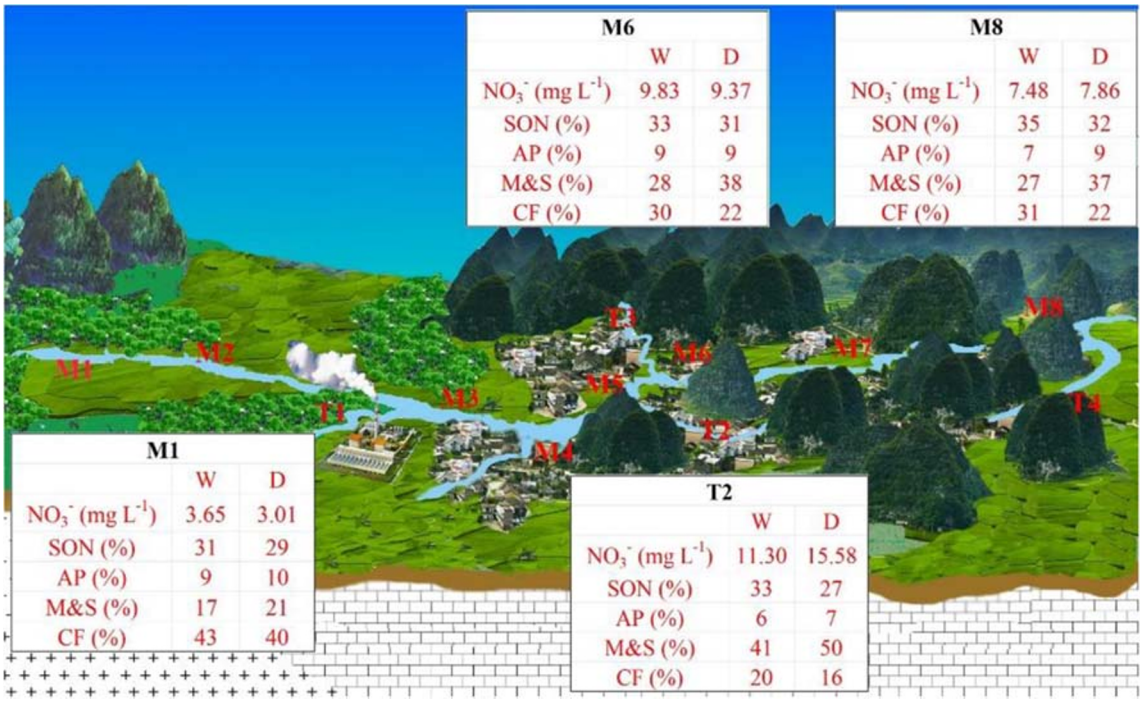

Fig. 7 Model diagram of NO_3^- concentration and main sources in the Lijiang River

smaller than 18.7% in small carbonate basin, Southwest China. This result indicates that carbon flux in rivers was impacted significantly by the nitrogen cycle, especially in this karst area, which should be considered for quantification of the carbon cycle. Hence, reducing nitrate inputs is important, especially NO_3^- from chemical fertilizer and sewage and manure.

Conclusions

In this study, the isotopic compositions of NO_3^- and H_2O and water chemistry data were used to elucidate the sources, transformations of NO_3^-, and analyze the influence of nitrogen cycling on the process of carbonate rock weathering of surface water in karst areas. The Bayesian model was employed to estimate the proportional contributions of the NO_3^- sources. According to the fingerprint feature ($\delta^{15}N\text{-}NO_3^-$ and $\delta^{18}O\text{-}NO_3^-$) of the nitrate sources, the main nitrate source is the SON, M&S, and CF for all water samples. The hydrochemical data and coupled isotopic compositions of NO_3^- and H_2O suggested that NO_3^- transformation is dominated by nitrification processes, the mixing process has more effect on NO_3^- transportation, and no obvious denitrification was observed. The results of SIAR model showed that NO_3^- sources contribution rates were in the order: SON > M&S > CF > AP and have significant spatio-temporal difference, indicating that NO_3^- in the Lijiang River is greatly affected by nitrification of SON, CF, and M&S. Nitrification of fertilizers, soil, and manure and sewage results a significant increase of the export of HCO_3^-, and the enhanced HCO_3^- flux caused by the nitrification could account for about 11% of the total HCO_3^- in the Lijiang River. NO_3^- discharge flux in the Lijiang River was 4.10×10^7 kg year^{-1}, and about 62% of which was derived from anthropogenic activities. Hence, fertilization and manure and sewage management control were important to reduce NO_3^- and HCO_3^- discharge flux in the Lijiang River.

Funding information This work was jointly supported by the National Key Research and Developmental Program of China (2016YFC0502306), the Special Fund for Basic Scientific Research of Chinese Academy of Geological Sciences (YYWF201639), the Basic Scientific Research of Chinese Academy of Geological Sciences (JYYWF20182002), the Guangxi Natural Science Foundation (2016GXNSFAA380064; 2018GXNSFDA050002), the National Natural Science Foundation of China (41472321), and the Chongqing Municipal Science and Technology Commission Fellowship Fund (CSTC2017jcyj-yszx0004; CSTC2018jcyj-yszx0013).

References

Andersson KK, Hooper AB (1983) O_2 and H_2O are each the source of one O in NO_2^- produced from NH_3 by Nitrosomonas: ^{15}N-NMR evidence. Fed Eur Biochem Soc 164:236–240. https://doi.org/10.1016/0014-5793(83)80292-0

Barkan E, Luz B (2005) High precision measurements of $^{17}O/^{16}O$ and $^{18}O/^{16}O$ ratios in H_2O. Rapid Commun Mass Spectrom 19:3737–3742. https://doi.org/10.1002/rcm.2250

Barnes RT, Raymond PA (2009) The contribution of agricultural and urban activities to inorganic carbon fluxes within temperate watersheds. Chem Geol 266:318–327. https://doi.org/10.1016/j.chemgeo.2009.06.018

Boshers D, Granger J, Tobias C, Böhlke JK, Smith RL (2019) Constraining the oxygen isotopic composition of nitrate produced by nitrification. Environ Sci Technol 53:1206–1216. https://doi.org/10.1021/acs.est.8b03386

Bu H, Song X, Zhang Y, Meng W (2017) Sources and fate of nitrate in the Haicheng River basin in Northeast China using stable isotopes of nitrate. Ecol Eng 98:105–113. https://doi.org/10.1016/j.ecoleng.2016.10.052

Casciotti KL, Sigman DM, Hastings MG, Böhlke JK, Hilkert A (2002) Measurement of the oxygen isotopic composition of nitrate in seawater and freshwater using the denitrifier method. Anal Chem 74:4905–4912. https://doi.org/10.1021/ac020113w

Chen F, Zhou X, Lao Q et al (2019) Dual isotopic evidence for nitrate sources and active biological transformation in the Northern South China Sea in summer. PLoS One 14:1–16. https://doi.org/10.1371/journal.pone.0209287

Comly HH (1945) Cyanosis in infants caused by nitrates in well water. J Am Med Assoc 129:112–116. https://doi.org/10.1001/jama.1945.02860360014004

Dalton R (1995) San Diego research body put under microscope on costs. Nature 377:4. https://doi.org/10.1038/377004b0

Deutsch B, Mewes M, Liskow I, Voss M (2006) Quantification of diffuse nitrate inputs into a small river system using stable isotopes of oxygen and nitrogen in nitrate. Org Geochem 37:1333–1342. https://doi.org/10.1016/j.orggeochem.2006.04.012

Ding J, Xi B, Gao R, He L, Liu H, Dai X, Yu Y (2014) Identifying diffused nitrate sources in a stream in an agricultural field using a dual isotopic approach. Sci Total Environ 484:10–18. https://doi.org/10.1016/j.scitotenv.2014.03.018

Ford DC, Williams P (2007) Karst hydrogeology and geomorphology.John Wiley & Sons Ltd: England; 576

Fukada T, Hiscock KM, Dennis PF, Grischek T (2003) A dual isotope approach to identify denitrification in groundwater at a river-bank infiltration site. Water Res 37:3070–3078. https://doi.org/10.1016/S0043-1354(03)00176-3

Gaillardet J, Dupré B, Louvat P, Allègre CJ (1999) Global silicate weathering and CO_2 consumption rates deduced from the chemistry of large rivers. Chem Geol 159:3–30. https://doi.org/10.1016/S0009-2541(99)00031-5

Gandois L, Perrin A-S, Probst A (2011) Impact of nitrogenous fertiliser-induced proton releaseon cultivated soils with contrasting carbonate contents: a column experiment. Geochim Cosmochim Acta 75:1175–1198. https://doi.org/10.1016/j.gca.2010.11.025

Ghodeif K, Wahaab R, Sorour S (2017) The impact of low-flow season on source drinking water quality, Rosetta branch, Egypt. J Water Sanit Hyg Dev 7:477–484. https://doi.org/10.2166/washdev.2017.158

He XY (2013) Study on the production and application situation of chemical fertilizer in Guangxi. Guangxi Univ, PhD Dissertation (in Chinese)

Jiang Y (2013) The contribution of human activities to dissolved inorganic carbon fluxes in a karst underground river system: evidence from major elements and $\delta^{13}C_{DIC}$ in Nandong, Southwest China. J Contam Hydrol 152:1–11. https://doi.org/10.1016/j.jconhyd.2013.05.010

Kaown D, Koh DC, Mayer B, Lee KK (2009) Identification of nitrate and sulfate sources in groundwater using dual stable isotope approaches for an agricultural area with different land use (Chuncheon, mid-eastern Korea). Agric Ecosyst Environ 32:223–231. https://doi.org/10.1016/j.agee.2009.04.004

Kelley CJ, Keller CK, Evans RD et al (2013) Nitrate-nitrogen and oxygen isotope ratios for identification of nitrate sources and dominant nitrogen cycle processes in a tile-drained dryland agricultural field. Soil Biol Biochem 57:731–738. https://doi.org/10.1016/j.soilbio.2012.10.017

Kendall C, Elliott EM, Wankel SD (2008) Tracing anthropogenic inputs of nitrogen to ecosystems. In: Stable isotopes in ecology and environmental science: second edition pp. 375–449. https://doi.org/10.1002/9780470691854.ch12

Lee K-S, Bong Y-S, Lee D, Kim Y, Kim K (2008) Tracing the sources of nitrate in the Han River watershed in Korea, using $\delta^{15}N\text{-}NO_3^-$ and $\delta^{18}O\text{-}NO_3^-$ values. Sci Total Environ 395:117–124. https://doi.org/10.1016/J.SCITOTENV.2008.01.058

Li C, Ji H (2016) Chemical weathering and the role of sulfuric and nitric acids in carbonate weathering: isotopes (^{13}C, ^{15}N, ^{34}S, and ^{18}O) and chemical constraints. J Geophys Res G Biogeosciences 121:1288–1305. https://doi.org/10.1002/2015JG003121

Li C, Li S, Yue F, Liu J, Zhong J, Yan ZF, Zhang RC, Wang ZJ, Xu S (2018) Identification of sources and transformations of nitrate in the Xijiang River using nitrate isotopes and Bayesian model. Sci Total Environ 646:801–810. https://doi.org/10.1016/j.scitotenv.2018.07.345

Lin P, Chen Y. (2016) Types and causes of water pollution under different land use types in Lijiang River Basin. J Guilin Univ Technol 36:539–544(in Chinese)

Liu C, Li S, Lang Y, Xiao H (2006) Using $\delta^{15}N$ and $\delta^{18}O$ values to identify nitrate sources in karst ground water, Guiyang, Southwest China. Environ Sci Technol 40:6928–6933. https://doi.org/10.1021/es0610129

Liu J, Shen Z, Yan T, Yang Y (2018a) Source identification and impact of landscape pattern on riverine nitrogen pollution in a typical urbanized watershed, Beijing, China. Sci Total Environ 628:1296–1307. https://doi.org/10.1016/j.scitotenv.2018.02.161

Liu S, Wu F, Feng W, Guo W, Song F, Wang H, Wang Y, He Z, Giesy JP, Zhu P, Tang Z (2018b) Using dual isotopes and a Bayesian isotope mixing model to evaluate sources of nitrate of Tai Lake, China. Environ Sci Pollut Res 25:32631–32639. https://doi.org/10.1007/s11356-018-3242-1

Lu L, Cheng H, Pu X, Liu X, Cheng Q (2015) Nitrate behaviors and source apportionment in an aquatic system from a watershed with intensive agricultural activities. Environ Sci Process Impacts 17:131–144. https://doi.org/10.1039/c4em00502c

Matiatos I (2016) Nitrate source identification in groundwater of multiple land-use areas by combining isotopes and multivariate statistical analysis: a case study of Asopos basin (Central Greece). Sci Total Environ 541:802–814. https://doi.org/10.1016/J.SCITOTENV.2015.09.134

Mayer B, Bollwerk SM, Mansfeldt T et al (2001) The oxygen isotope composition of nitrate generated by nitrification in acid forest floors. Geochim Cosmochim Acta 65:2743–2756. https://doi.org/10.1016/S0016-7037(01)00612-3

Moore JW, Semmens BX (2008) Incorporating uncertainty and prior information into stable isotope mixing models. Ecol Lett 11:470–480. https://doi.org/10.1111/j.1461-0248.2008.01163.x

NBSC, National Bureau of Statistics (NBS) of China (Ed.), 1980-2018. China statistical yearbook. China Science ans Technology Press http://www.stats.gov.cn

Ogrinc N, Tamše S, Zavadlav S, Vrzel J, Jin L (2019) Evaluation of geochemical processes and nitrate pollution sources at the Ljubljansko Polje aquifer (Slovenia): a stable isotope perspective. Sci Total Environ 646:1588–1600. https://doi.org/10.1016/J.SCITOTENV.2018.07.245

Parnell AC, Inger R, Bearhop S, Jackson AL (2010) Source partitioning using stable isotopes: coping with too much variation. PLoS One 5:1–5. https://doi.org/10.1371/journal.pone.0009672

Parnell AC, Phillips DL, Bearhop S et al (2013) Bayesian stable isotope mixing models. Environmetrics 24:387–399. https://doi.org/10.1002/env.2221

Pastén-Zapata E, Ledesma-Ruiz R, Harter T, Ramírez AI, Mahlknecht J (2014) Assessment of sources and fate of nitrate in shallow groundwater of an agricultural area by using a multi-tracer approach. Sci

Total Environ 470–471:855–864. https://doi.org/10.1016/J.SCITOTENV.2013.10.043

Pernet-Coudrier B, Qi W, Liu H, Müller B, Berg M (2012) Sources and pathways of nutrients in the semi-arid region of Beijing-Tianjin, China. Environ Sci Technol 46:5294–5301. https://doi.org/10.1021/es3004415

Perrin A-S, Probst A, Probst J-L (2008) Impact of nitrogenous fertilizers on carbonate dissolution in small agricultural catchments: implications for weathering CO_2 uptake at regional and global scales. Geochim Cosmochim Acta 72:3105–3123. https://doi.org/10.1016/j.gca.2008.04.011

Qin X, He B, Shen L, Wang K, Yu Q (2018) Characteristics of soil and water loss in the Lijiang River Basin and soil erosion factors in typical karst small watersheds. Carsol Sin 37:351–360 (in Chinese)

Qin Y, Zhang D, Wang F (2019) Using nitrogen and oxygen isotopes to access sources and transformations of nitrogen in the Qinhe Basin, North China. Environ Sci Pollut Res 26:738–748. https://doi.org/10.1007/s11356-018-3660-0

Raymond PA, Oh NH, Turner RE, Broussard W (2008) Anthropogenically enhanced fluxes of water and carbon from the Mississippi River. Nature 451:449–452. https://doi.org/10.1038/nature06505

Rivett MO, Buss SR, Morgan P, Smith JW, Bemment CD (2008) Nitrate attenuation in groundwater: a review of biogeochemical controlling processes. Water Res 42:4215–4232. https://doi.org/10.1016/j.watres.2008.07.020

Saccon P, Leis A, Marca A et al (2013) Multi-isotope approach for the identification and characterisation of nitrate pollution sources in the Marano lagoon (Italy) and parts of its catchment area. Appl Geochem 34:75–89. https://doi.org/10.1016/j.apgeochem.2013.02.007

Shen H, Jiang G, Guo F et al (2015) Distribution characteristics and influence factors of the ammoia, nitrite and nitrate in the Lijiang River,Guilin City. Carsologica Sin 34:369–374 (in Chinese)

Sigman DM, Granger J, Difiore PJ et al (2005) Coupled nitrogen and oxygen isotope measurements of nitrate along the eastern North Pacific margin. Global Biogeochem Cycles:19. https://doi.org/10.1029/2005GB002682

Sigman DM, Lehmann MF, Tortell PD et al (2008) Nitrogen and oxygen isotope fractionation during dissimilatory nitrate reduction by denitrifying bacteria. Limnol Oceanogr 53:2533–2545

Soto DX, Koehler G, Wassenaar LI, Hobson KA (2019) Spatio-temporal variation of nitrate sources to Lake Winnipeg using N and O isotope ($\delta^{15}N$, $\delta^{18}O$) analyses. Sci Total Environ 647:486–493. https://doi.org/10.1016/j.scitotenv.2018.07.346

Van Beek LPH, Middelburg JJ, Bouwman AF et al (2016) Global riverine N and P transport to ocean increased during the 20th century despite increased retention along the aquatic continuum. Biogeosciences 13:2441–2451. https://doi.org/10.5194/bg-13-2441-2016

Widory D, Petelet-Giraud E, Négrel P, Ladouche B (2005) Tracking the sources of nitrate in groundwater using coupled nitrogen and boron isotopes: a synthesis. Environ Sci Technol 39:539–548. https://doi.org/10.1021/es0493897

Xian C, Ouyang Z, Li Y, Ren Y (2016) Variation in nitrate isotopic signatures in sewage for source apportionment with urbanization: a case study in Beijing, China. Environ Sci Pollut Res 23:22871–22881. https://doi.org/10.1007/s11356-016-7498-z

Xue D, Botte J, De Baets B et al (2009) Present limitations and future prospects of stable isotope methods for nitrate source identification in surface- and groundwater. Water Res 43:1159–1170. https://doi.org/10.1016/j.watres.2008.12.048

Xue D, De Baets B, Van Cleemput O et al (2012) Use of a Bayesian isotope mixing model to estimate proportional contributions of multiple nitrate sources in surface water. Environ Pollut 161:43–49. https://doi.org/10.1016/j.envpol.2011.09.033

Yuan YQ (2016) Impacts of aquatic organisms on hydrochemical characteristics and karst carbon sink in Lijiang Basin. Guangxi Univ, PhD Dissertation (in Chinese)

Yue FJ, Li SL, Liu CQ et al (2015) Sources and transport of nitrate constrained by the isotopic technique in a karst catchment: an example from Southwest China. Hydrol Process 29:1883–1893. https://doi.org/10.1002/hyp.10302

Zhang M, Zhi Y, Shi J, Wu L (2018) Apportionment and uncertainty analysis of nitrate sources based on the dual isotope approach and a Bayesian isotope mixing model at the watershed scale. Sci Total Environ 639:1175–1187. https://doi.org/10.1016/j.scitotenv.2018.05.239

Zhang T, Li J, Pu J, Martin JB, Khadka MB, Wu F, Li L, Jiang F, Huang S, Yuan D (2017) River sequesters atmospheric carbon and limits the CO_2 degassing in karst area, Southwest China. Sci Total Environ 609:92–101. https://doi.org/10.1016/j.scitotenv.2017.07.143

Zong Z, Wang X, Tian C, Chen Y, Fang Y, Zhang F, Li C, Sun J, Li J, Zhang G (2017) First assessment of NOx sources at a regional background site in North China using isotopic analysis linked with modeling. Environ Sci Technol 51:5923–5931. https://doi.org/10.1021/acs.est.6b06316